



HYDROTHERMAL SYNTHESIS OF TiO_2 NANOPARTICLES FOR ANTIBACTERIAL ACTIVITY

Gopala Krishna Murthy HR¹, Sanjeevarayappa C²

¹Associate Professor, GFGC, Nanjangud, Mysuru, Karnataka, India.; gkmurthyy123@gmail.com;

²Associate Professor, GFGC, Yelahanka, Karnataka, India.

Abstract

Green synthesis has emerged as a non-toxic, economical, and environmentally benign approach for the fabrication of nanoparticles, offering a sustainable alternative to conventional chemical and physical methods. Among various synthesis routes, hydrothermal synthesis is one of the most widely employed techniques for nanomaterial preparation due to its simplicity, high efficiency, and ability to produce materials over a wide temperature range, from ambient to elevated conditions. Titanium dioxide nanoparticles (TiO_2 NPs) have gained significant attention because of their diverse applications, particularly in agriculture, environmental remediation, and biomedical fields. TiO_2 NPs play an important role in enhancing plant growth and improving plant tolerance against abiotic stress. In the present study, TiO_2 nanoparticles were successfully green synthesized using an aqueous leaf extract of *Erythrina variegata*, which acts as both a reducing and capping agent, facilitating the conversion of metal precursors into stable metal-oxide nanoparticles. The UV–Vis spectrum exhibited a characteristic absorption band at 319.2 nm, confirming TiO_2 NP formation, with an optical band-gap energy of 2.41 eV. XRD analysis confirmed the crystalline and pure nature of the synthesized nanoparticles. Furthermore, the green-synthesized TiO_2 NPs demonstrated excellent photocatalytic degradation of methylene blue dye under UV irradiation and exhibited notable antibacterial activity against both Gram-positive and Gram-negative pathogenic bacteria, highlighting their multifunctional potential.

IndexTerms: Synthesis, TiO_2 , Antibacterial;

1. INTRODUCTION

Nanotechnology involves the design and development of materials at the nanoscale, typically in the size range of 1–100 nm, where materials exhibit unique physical, chemical, and optical properties compared to their bulk counterparts [1,3]. These changes arise mainly due to high surface area, small particle size, and enhanced reactivity, making nanomaterials highly useful in various applications such as healthcare, environmental remediation, and energy systems [3,4].

Nanoparticles are broadly classified into organic nanoparticles, including liposomes, micelles, and chitosan, and inorganic nanoparticles such as metallic, magnetic, and metal-oxide nanoparticles [3]. In recent decades, nanomaterials have gained significant global attention due to their efficiency as photocatalysts for the degradation of antibiotics and organic pollutants [7,8].

Among metal-oxide nanomaterials, titanium dioxide (TiO_2) is one of the most extensively studied materials due to its wide range of applications in photocatalysis, dye-sensitized solar cells, sensors, and electrochromic devices [4,7]. A material is considered electrochromic when it shows a reversible change in optical properties due to electrochemically induced redox reactions [12]. TiO_2 is regarded as an electro-active material because of its high electrochromic activity, strong oxidation capability, and excellent chemical stability [4].

TiO_2 exists in different crystalline phases, mainly anatase and rutile, with anatase being more photocatalytically active and rutile being thermodynamically stable at high temperatures [4,12]. Titanium dioxide nanoparticles are preferred due to their low cost, chemical stability, and strong oxidizing power [5,6]. As an n-type semiconductor with a wide band gap of about 3.2 eV, TiO_2 primarily absorbs UV light and is widely used for the photocatalytic degradation of organic pollutants and antibiotics [7,10].

2. Materials and Methods

Plant material: Leaves of *E. variegata* are gathered from garden of the Mysuru, Karnataka, India and dried in shade. Plant material is powdered and stored in air-tight container at room temperature.

Chemicals: Titanium tetraisopropoxide (TTIP, Sigma Aldrich, ARgrade,

Plant extract preparation: *E. variegata* leaves are washed many times then leaves are dried in the shade at room temperature for 10 days. The dried leaves are made to fine powder. The aqueous extract is organized through Soxhlet extraction method. The 15g of dried leaf powder of plant material is loaded into thimble placed inside Soxhlet extractor. The solvent is heated and evaporated at 100°C. The condensate is poured in dropped into flask and cycle started again. The process runs for total of 6 hours. the fine extract different natural compounds is filtered through Whatmann No.1 filter paper and stored safely for future purpose.

2.1 Synthesis of TiO_2 NPs

TTIP (1N) is prepared through distilled water. 20 ml of *E. variegata* extract is inserted to 0.1 N TTIP solutions. Figure 1 describes the titanium dioxide (TiO_2) nanoparticles (NPs) synthesis using *Erythrina variegata* leaves.

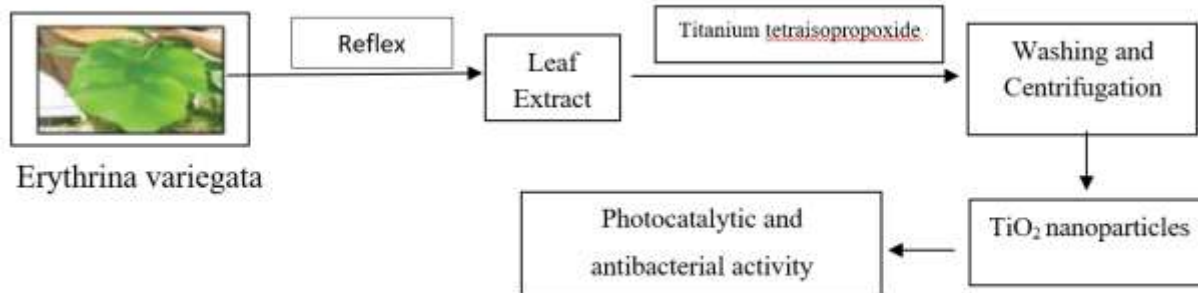


Figure 1: Titanium Dioxide (TiO_2) Nanoparticles (NPs) Synthesis

The pale yellow slowly turned to sandal color after 6 hour of continuous stirring. The color change is due to formation of TiO_2 NPs. The synthesized NPs are separated through centrifuging and dried in hot air oven at 90 °C for 7 hours. NPs are classified through UV-Vis spectrum, FTIR and XRD.

2.2 Characterization of TiO_2 NPs

The color variation in reaction mixture examined. The absorption maxima in UV-Vis are computed using double-beam spectrophotometer in range between 200 nm - 900 nm through distilled water as reference. FTIR spectrum of TiO_2 NPs is recorded using FTIR spectrophotometer. The functional groups exist in the samples are identified with the FTIR spectral data. The sample is prepared as 0.25 mm thick KBr pellets. The spectrum is recorded between 4000 - 400 cm^{-1} nm. XRD patterns are achieved for powder samples. Phase purity and size are determined through XRD analysis.

2.3 Photocatalytic Activity of TiO_2 NPs

The photocatalytic degradation is performed using green-synthesized TiO_2 NPs in UV light. In the experimental study, a suspension is prepared by mixing 0.02 mg of TiO_2 NPs to 100 ml of 10 ppm methylene blue solution. The mixture is stirred for about 30 minutes. Degradation is visually identified through change in color of dye solution from deep blue to colorless. Simultaneously, the absorbance of dye solution before and after degradation by TiO_2 NPs at regular time intervals of exposure to UV light is determined.

2.4. Antibacterial activity of TiO₂ NPs

The antibacterial activity of *E. variegata* leaf extract TiO₂ NPs is examined Disc-diffusion method against the pathogenic organisms like *Staphylococcus* and *E. coli*. The results were predicted based on the zone of inhibition.

3. Results and Discussion

The performance of the TiO₂ nanoparticles synthesis is examined with Hydrothermal Synthesis method. The results of different synthesis methods are analyzed with different TiO₂ characterization are visual observations, X-ray diffraction [XRD], Fourier transform infrared [FTIR] and UV-Visible spectroscopy [UV-Vis] along with Antibacterial activity of TiO₂ NPs.

3.1 UV-Vis spectral studies:

The fundamental characterization of TiO² nanoparticles is performed using UV-visible spectroscopy. UV-Vis spectra of TiO₂ NPs are recorded using the double-beam spectrophotometer in range 200 to 900 nm.

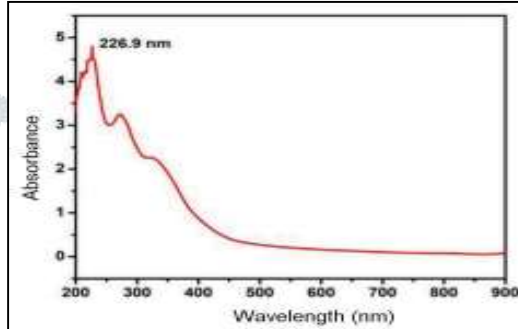


Figure 2: UV-Visible Spectrum of *Erythrina Variegata* Leaves

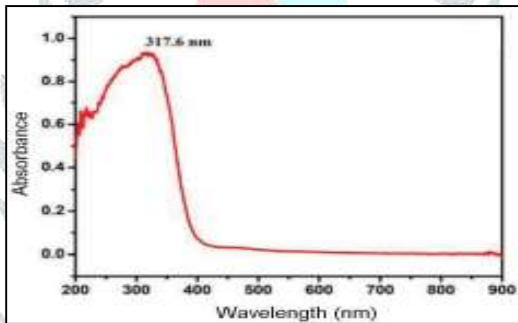


Figure 3: UV-Visible Spectrum of Synthesized TiO² NPs

Figure 2 and 3 shows the absorption spectrum of aq. extract of *E. variegata* leaves and the synthesized TiO₂ NPs. As shown in the above graphical plot, the vertical axis represents absorbance and the horizontal axis represents the wavelength [nm]. The absorption maximum at 320 nm supports the formation of TiO² NPs.

3.2 FTIR spectral studies

FTIR is a method used to attain the infrared spectrum of absorption of synthesized TiO₂ nanoparticles. FTIR spectrometer gives the high-resolution spectral data and determines the intensity range of wavelength. FTIR spectral analysis is performed to find the functional groups of molecules bound particularly along TiO₂ NPs surface.

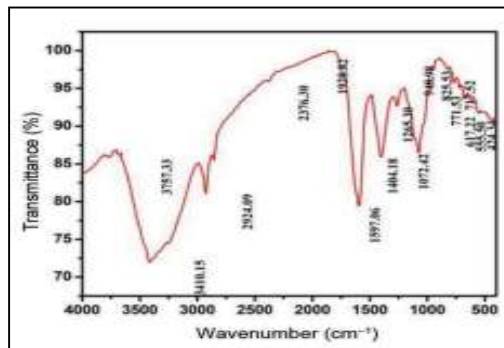


Figure 4: FTIR Spectra of Erythrina Variegata Leaf Extract

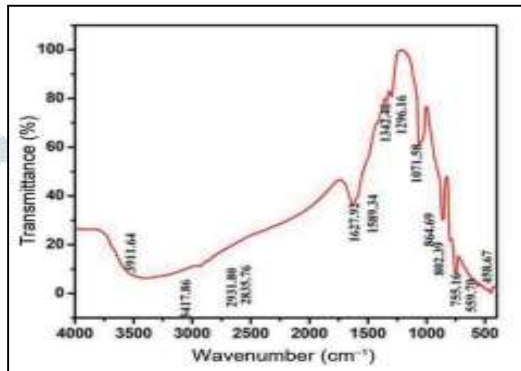


Figure 5: FTIR Spectra of TiO₂ NPs

Figure 4 and 5 describes the FTIR spectra of leaf powder extract of *E.variegata* and TiO₂ NPs. In the above graphical plot, the vertical axis represents Transmittance (%) and the horizontal axis represents the wave number [cm⁻¹]. The spectrum is recorded in the range 4000 to 400 cm⁻¹. The peaks at 3400 cm⁻¹ and 1600 cm⁻¹ is because of OH stretching and bending vibration of surface-adsorbed water correspondingly. The hydroxyl group bound to surface of TiO₂ is used to trigger the photocatalytic activity of NPs. FTIR spectrum of green synthesize NPs showed characteristic bands at 2800 cm⁻¹ representing the secondary amines and 2915 cm⁻¹ verifying hydrogen bonded alcohols. The strong peak observed at 1615 cm⁻¹ denoted aliphatic of nitro compound with stretching of NO and peak at 1050 cm⁻¹ denoted ether. The absorption band with stretching mode of Ti-O in fingerprint region 750 cm⁻¹ correspond to anatase phase of TiO₂. FTIR results verified the formation of anatase TiO₂ because of TTIP precursor reduction through phytochemical components in extract of *E.V.* leaves. The components included many organic functional groups attached to surface of TTIP and cause reduction. The component functioned as the good reducing and capping agents.

3.3 X-Ray Diffraction Studies

X-ray diffraction [XRD] pattern of CeO₂ nanoparticles characterization is carried out by using Hydrothermal Synthesis method. X-ray diffraction analysis is a method used in nanotechnology to determine the crystallographic structure of TiO₂ nanoparticles. The average size of TiO₂ NPs is calculated using the Debye-Scherrer equation. The TiO₂ nanoparticles crystallite size in XRD pattern is calculated by using formula,

$$\text{crystallite size (S)} = \frac{k * \lambda_{\text{xray}}}{b * \cos \theta} \quad (1)$$

From (1), 'k' represent the constant depending on the crystallite size. 'λ_{xray}' symbolize the wavelength of X-ray, 'b' denotes the full width half maximum in radians, 'θ' denotes the peak position in degree.

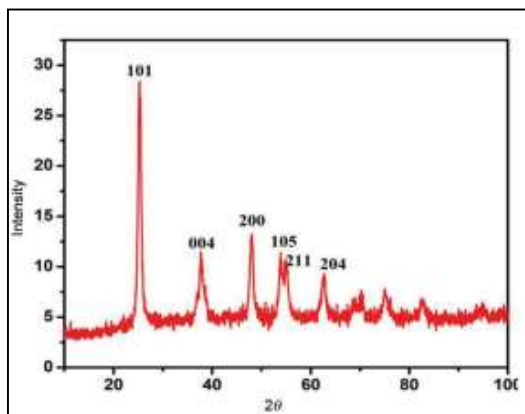


Figure 6: X-ray diffraction pattern of TiO_2 NPs

Figure 6 shows the XRD pattern of synthesized TiO_2 NPs. The peak appearing at 2θ values of 26.20° , 36.50° , 49.10° , 54.90° , 54.65° and 61.12° correspond to the Bragg reflection of (101), (004), (200), (105), (211) and (204) planes correspondingly. The diffraction peaks denote the tetragonal body-centered structure of TiO_2 NPs. Sharp and broad diffraction peaks are observed to level crystallinity and nanosized crystallite. The data are in good agreement with JCPDS card no. 84-1285.

3.4 Antibacterial activity of TiO_2 NPs

The antibacterial action of green-synthesized TiO_2 NPs is examined for 4 diverse pathogenic strains, namely *Streptococcus*, *Staphylococcus*, *E. coli* and *P. aeruginosa*. With help of disk diffusion technique, inhibition zones for Gram-positive and Gram-negative bacteria.

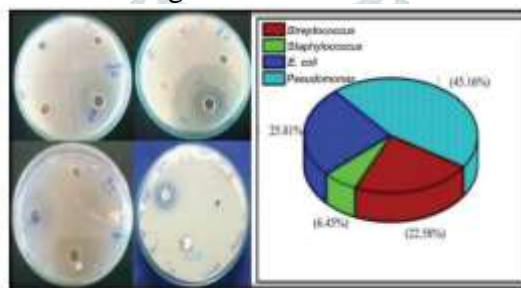


Figure 7: Antibacterial Activity

Figure 7 explains the diffusion assay to assess the bactericidal of biosynthesized TiO_2 NPs obtained from *Erythrina variegata* leaf extract against different bacterial strains, namely *Streptococcus*, *Staphylococcus*, *Staphylococcus aureus*, *Escherichia coli* and *Pseudomonas aeruginosa*

4. Conclusion

In this study, an eco-friendly green hydrothermal method was successfully employed for the synthesis of titanium dioxide (TiO_2) nanoparticles using *Erythrina variegata* leaf extract. The plant extract acted as a natural reducing and stabilizing agent, enabling the efficient conversion of titanium tetraisopropoxide into TiO_2 nanoparticles within a short reaction time [2,6,10]. The green hydrothermal approach proved to be safe, cost-effective, and environmentally benign compared to conventional synthesis techniques [3,9].

The formation of TiO_2 nanoparticles was initially confirmed by a visible color change of the precipitate from pale yellow to sandal color. UV-Vis spectroscopy showed a characteristic absorption peak at 322.1 nm, confirming nanoparticle formation, while the optical band gap was determined to be 2.36 eV using Tauc plot analysis [4,7]. XRD analysis confirmed the crystalline nature and purity of the synthesized TiO_2 nanoparticles [9,10].

Overall, the results demonstrate that the green hydrothermal synthesis method offers better performance in terms of reaction time, simplicity, and sustainability, making it a promising approach for large-scale synthesis and potential biomedical and environmental applications [11,12].

References

[1] Reddy, K. M.; Feris, K.; Bell, J.; Wingett, D. G.; Hanley, C.; Punnoose, A. Selective toxicity of zinc oxide nanoparticles to prokaryotic and eukaryotic systems. *Applied Physics Letters*, 90, 213902 (2007). DOI: 10.1063/1.2742324

[2] Santhoshkumar, T.; Rahuman, A. A.; Kumar, K.; Marimuthu, S.; Jayaseelan, C.; Ramkumar, L. Green synthesis of TiO₂ nanoparticles using plant extracts and their antibacterial activity. *Journal of Photochemistry and Photobiology B: Biology*, 130, 49–56 (2014). DOI: 10.1016/j.jphotobiol.2013.10.015

[3] Mittal, A. K.; Chisti, Y.; Banerjee, U. C. Biosynthesis of metallic nanoparticles using plant extracts: A review. *Journal of Nanoparticle Research*, 15, 1414 (2013). DOI: 10.1007/s11051-012-1414-8

[4] Chen, X.; Mao, S. S. Titanium dioxide nanomaterials: Synthesis, properties, modifications, and applications. *Chemical Reviews*, 107, 2891–2959 (2007). DOI: 10.1021/cr0500535

[5] Banerjee, S.; Gopalakrishnan, C.; Rajeshkumar, S.; Paul, N.; Abraham, J. TiO₂ nanoparticles and their antibacterial activity. *Materials Science and Engineering: C*, 30, 248–254 (2010). DOI: 10.1016/j.msec.2009.11.014

[6] Rajakumar, G.; Arockiaraj, J.; Paulraj, R.; Ranjithkumar, R.; Kalamani, T.; John, S. A. Green synthesis of TiO₂ nanoparticles using plant leaf extract and their antimicrobial properties. *Spectrochimica Acta Part A: Molecular and Biomolecular Spectroscopy*, 118, 739–744 (2014). DOI: 10.1016/j.saa.2013.09.040

[7] Fujishima, A.; Rao, T. N.; Tryk, D. A. Titanium dioxide photocatalysis. *Journal of Photochemistry and Photobiology C: Photochemistry Reviews*, 1, 1–21 (2000). DOI: 10.1016/S1389-5567(00)00002-2

[8] Ibadon, A. O.; Fitzpatrick, P.; Heterogeneous photocatalysis: Recent advances and applications. *Catalysts*, 3, 189–218 (2013). DOI: 10.3390/catal3010189

[9] Natarajan, S.; Rajendran, V.; Philip, J.; Mathews, T.; Hydrothermal synthesis and characterization of TiO₂ nanoparticles. *Materials Letters*, 64, 2420–2423 (2010). DOI: 10.1016/j.matlet.2010.07.080

[10] Prakash, J.; Ansari, S. A.; Al-Assiri, M. S.; Shaikh, S. F.; Tiwari, A.; Jadhav, S.; Plant-mediated green synthesis of TiO₂ nanoparticles and their photocatalytic activity. *Journal of Environmental Chemical Engineering*, 4, 2563–2571 (2016). DOI: 10.1016/j.jece.2016.04.020

[11] Moritz, M.; Geszke-Moritz, M.; The newest achievements in synthesis, immobilization, and practical applications of antibacterial nanoparticles. *Chemical Engineering Journal*, 228, 596–613 (2013). DOI: 10.1016/j.cej.2013.05.046

[12] Carp, O.; Huisman, C. L.; Reller, A.; Photoinduced reactivity of titanium dioxide. *Progress in Solid State Chemistry*, 32, 33–177 (2004). DOI: 10.1016/j.progsolidstchem.2004.08.001